

Better tired than lost: turtle ant trail networks favor coherence over shortest paths

Arjun Chandrasekhar¹, James A. R. Marshall², Cortnea Austin³, Saket Navlakha^{1*}, Deborah M. Gordon^{4*}

*For correspondence:

dmgordon@stanford.edu (DMG);
navlakha@salk.edu (SN)

¹Integrative Biology Laboratory, Salk Institute for Biological Studies, La Jolla, CA 92037;

²Department of Computer Science, University of Sheffield, Sheffield, UK; ³Central Washington University, Ellensburg, WA 98926; ⁴Department of Biology, Stanford University, Stanford CA 94305

1

2 Abstract

3 Creating a routing backbone is a fundamental problem in both biology and engineering. The
4 routing backbone of arboreal turtle ants (*Cephalotes goniodontus*) connects many nests and food
5 sources using trail pheromone. Unlike species that forage on the ground, arboreal ants are
6 constrained to form trail networks along branches and vines within the vegetation. We examined
7 what objectives the ant networks meet by comparing the observed turtle ant trail networks with
8 alternative networks of random, hypothetical trails in the same surrounding vegetation. We found
9 that turtle ant trail networks favor coherence, keeping the ants together on the trails, rather than
10 minimizing the distance traveled along edges in the graph. The ants' trails minimized the number
11 of nodes traversed, reducing the opportunity for ants to get lost at each node, and favored nodes
12 with 3D configurations most easily reinforced by pheromone, reducing the opportunities for ants to
13 diverge onto different paths. Thus, rather than forming the shortest paths, the ant networks take
14 advantage of natural variation in the environment to promote the maintenance of a coherent trail
15 that ensures that ants stay connected along the routing backbone.

16

17 **Keywords:** *Cephalotes*, ant trail network, routing networks, foraging, distributed algorithms,
18 search, exploration, shortest path, spanning tree

19 Introduction

20 Many engineered systems rely on a backbone routing network, whose goal is to ensure that
21 any two entities or devices on the network can communicate through some path (*Lynch, 1996*;
22 *Alwan and Agarwal, 2009*; *Chouikhi et al., 2015*). Some biological systems, such as neural ar-
23 bors (*Chandrasekhar and Navlakha, 2019*), plant arbors (*Conn et al., 2017*), and slime molds (*Tero
24 et al., 2010*), also use routing networks, to transmit information and nutrients. Effective design of
25 routing networks depends on the physical environment, because variation in the environment can
26 affect the accuracy and rate of communication in both engineered (*Fei et al., 2016*; *Nguyen and Xu,
27 2007*; *Gong et al., 2016*) and evolved natural networks (*Levin, 2016*; *Wiles et al., 2016*; *Hein et al.,
28 2016*; *Couzin et al., 2005*). The environment influences how the system chooses search strategies,
29 prioritizes competing objectives, and coordinates its local decisions. For example, wireless networks
30 operating in difficult to reach environments may use different routing strategies to minimize energy

31 consumption of devices (**Fei et al., 2016**); similarly, in bacterial navigation, chemicals appearing as
32 localized pulses in the environment can affect gradient sensing and movement patterns (**Hein et al.,**
33 **2016**).

34 The 14,000 species of ants have evolved diverse distributed routing algorithms to search for,
35 obtain, and distribute resources (**Gordon, 2014, 2016**) in diverse environments (**Dussutour et al.,**
36 **2004; Latty et al., 2011; Middleton and Latty, 2016; Gordon, 2019; Perna and Latty, 2014**). Models
37 of engineered routing networks inspired by ants often emphasize the goal of minimizing the distance
38 traveled. Ant colony optimization (ACO), first proposed in 1991, loosely mimics ant behavior to
39 solve combinatorial optimization problems, such as the traveling salesman problem (**Colorni et al.,**
40 **1991; Dorigo and Blum, 2005; López-Ibáñez et al., 2015**) and other such routing problems (**Di Caro**
41 **and Dorigo, 1998**). In ACO, individual ants each use a heuristic to construct candidate solutions, and
42 then use pheromone to lead other ants towards better solutions. Recent advances improve ACO
43 through techniques such as local search (**Gambardella et al., 2012**), cunning ants (**Tsutsui, 2007**),
44 and iterated ants (**Wiesemann and Stützle, 2006**).

45 A fascinating recent area of biological research examines the goals met by the trail networks of
46 ants (**Perna and Latty, 2014**). Studies of species that forage on a continuous 2D surface (**Middleton**
47 **and Latty, 2016**), including Pharaoh's ants (**Malíčková et al., 2015**), Argentine ants (**Latty et al.,**
48 **2011; Flanagan et al., 2013; Garnier et al., 2009**), leaf-cutter ants (**Dussutour et al., 2004**), army
49 ants (**Deneubourg et al., 1989; Couzin and Franks, 2003**), red wood ants (**Cherix et al., 1980**), and
50 meat ants (**Cabanes et al., 2014; Bottinelli et al., 2015**), show that ants use local chemical inter-
51 actions to form trails (**Deneubourg et al., 1986; Franks, 1989; Deneubourg et al., 1989**), regulate
52 traffic flow (**Bouchebti et al., 2019**), search collectively (**Countryman et al., 2015**), and form living
53 bridges (**Garnier et al., 2013**).

54 There are many objectives that an ant colony's trail network might meet, including minimizing
55 energy costs by reducing the distance traveled, keeping the ants together to form a coherent trail,
56 resilience to rupture, and effective searching (**Cook et al., 2014**). Ant species that forage and build
57 trails on the ground have few constraints on trail geometry because their trails can form nodes and
58 edges anywhere on the 2D plane. Prior work (**Aron et al., 1989; Garnier et al., 2009; Cook et al.,**
59 **2014**) showed that ground-living ants, such as red wood ants and Argentine ants, may minimize
60 the distance traveled by forming trails with branch points that approximate 2D Steiner trees (**Latty**
61 **et al., 2011; Buhl et al., 2009; Prömel and Steger, 2012**). However, minimizing distance may not
62 be the only objective that ant trail networks attempt to optimize. Army ants link their bodies to
63 form a bridge across gaps, but may not form the shortest possible bridge if this requires the use
64 of more ants (**Reid et al., 2015**). Meat ants form trail networks that link nests and trees as nodes,
65 and their choices of which nodes are linked, as well as the direction and length of trails, suggest
66 that robustness to the loss of a node is as important as minimizing the distance traveled (**Bottinelli**
67 **et al., 2015; Cabanes et al., 2014**).

68 Many ant species operate in 3D environments, such as arboreal ants that nest and forage in
69 trees and bushes. Unlike species that have evolved to create graph structures in continuous space
70 in an unconstrained 2D plane, arboreal ants must solve problems on a natural graph structure.
71 They cannot form trails with nodes and edges at arbitrary locations; instead, they can use only
72 the nodes and edges that are available to them. The arboreal turtle ant (*Cephalotes goniodontus*)
73 nests and forages in the tree canopy of tropical forests (**Powell et al., 2011**). A turtle ant colony
74 creates a trail network in the vegetation that connects several nests, providing a routing backbone
75 that must be maintained to allow resources to be distributed throughout the colony (**Gordon, 2012,**
76 **2017**). Ants search off the backbone to find and create trails to ephemeral food sources. The colony
77 modifies the trail from day to day, sometimes forming small alternative paths, or loops, of which
78 one is eventually chosen. The colony repairs the backbone in response to frequent changes in
79 the vegetation caused by plant growth and by ruptures made by wind or passing animals (**Gordon,**
80 **2017**).

81 Results

82 Candidate objectives

83 Here we mapped trail networks of turtle ants in their natural habitat and computationally tested
84 what objective functions these trails may be optimizing. We compared the observed networks with
85 simulated random networks, to determine how well the observed networks meet three objectives,
86 possibly in combination (*Bottinelli et al., 2015*):

87

88 1. Minimizing the distance traveled, which was measured as the average length of the edges
89 in the trail network. This is equivalent to minimizing the total trail length for a fixed number of
90 edges. Minimizing the distance traveled minimizes the energy cost of building the trail network.
91 This distance, however, is not equivalent to the number of nodes traversed, as is often assumed
92 in various optimization algorithms (*Dorigo and Stützle, 2004; Di Caro and Dorigo, 1998; Eberhart
93 et al., 1995; Karaboga, 2005*), including our previous work on turtle ants (*Chandrasekhar et al.,
94 2018*), because in the vegetation, the lengths of edges vary; the distance between one node and
95 another ranges from less than a centimeter to more than a meter (Table 1).

96

97 2. Minimizing the total number of nodes, which promotes the maintenance of a coherent trail
98 by reducing opportunities for ants to get lost, but also reduces the opportunities for exploration
99 and thus for finding new resources off the trail. The number of nodes was measured by counting
100 the nodes traversed along edges used in the trail network. We previously studied how ants at
101 a node select which transition through a node to traverse based on the rate at which volatile
102 pheromone is deposited (*Chandrasekhar et al., 2018*). Simulation results were consistent with
103 field observations (*Gordon, 2012*) indicating that ants at a node have a constant probability of
104 exploring, or taking a path that is not the one most strongly reinforced by pheromone, of about
105 0.2 per node (*Chandrasekhar et al., 2018*). Thus each node presents an opportunity for ants to get
106 lost, and lost ants may lay pheromone trail that could lead other ants astray. Each node is also an
107 opportunity to meet the ants of other colonies that make trails in the same vegetation. We test here
108 the hypothesis, indicated by previous observations (*Gordon, 2017*), that modification and repairs
109 to the backbone tend to reduce the number of nodes over time.

110

111 3. Minimizing the difficulty of establishing a pheromone trail by finding trajectories through nodes
112 that are most easily reinforced by pheromone. This objective also contributes to the creation
113 and maintenance of a coherent trail. We hypothesized that the physical configuration of a node
114 influences how likely are successive ants to cross the node in the same way, thus reinforcing it with
115 volatile trail pheromone. The ants have short antennae that detect pheromone only locally, so the
116 transition from one edge through a node to another edge is reinforced only when successive ants
117 take exactly the same trajectory through the node (Figure 1). Nodes are variable 3D structures,
118 ranging from a simple fork created by a branch in a plant, to a cluster of entwined vines and
119 branches from different plants. We used an arbitrary categorical index to estimate how many
120 possible trajectories an ant could take from one edge through a node to another edge, and thus
121 how likely a node is to be reinforced (Figure 1, details below). We tested whether the ants' behavior
122 reflected this estimate. Our previous work (*Gordon, 2017; Chandrasekhar et al., 2018*) did not take
123 into account variation among nodes, and did not examine how trails are selected from among the
124 many available alternative networks.

125 Preference for nodes more likely to be reinforced was measured as the average *transition index*
126 of all transitions in the trail network. The transition index is a categorical value that ranged from
127 1, where successive ants are most likely to take and reinforce the same trajectory through the
128 transition, to 4, where successive ants are least likely to take and reinforce the same trajectory
129 through the transition (Figure 1). The value of the transition index was assigned based on a visual
130 estimate of the number of different trajectories available for ants to traverse the node, drawing on

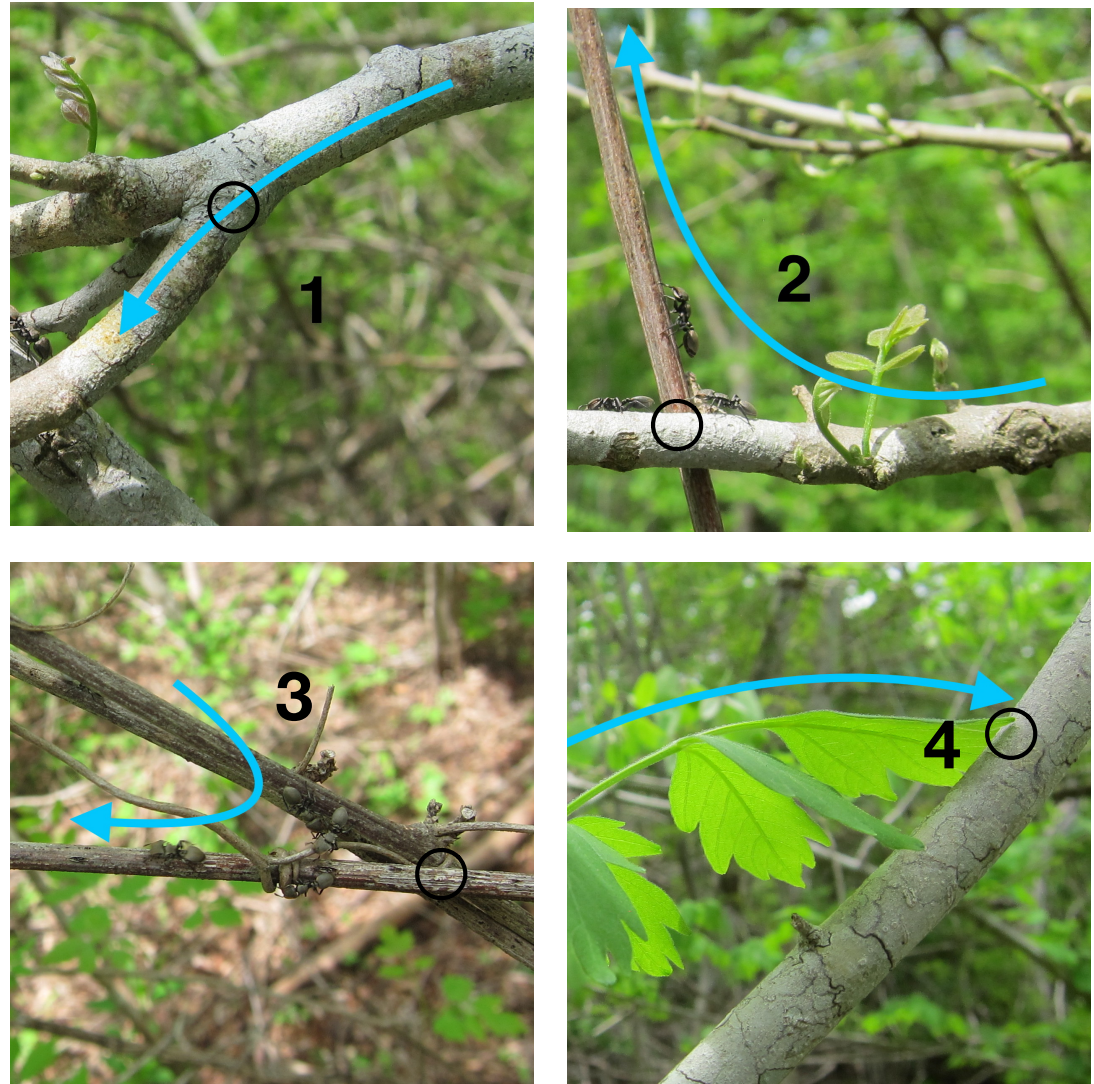


Figure 1. Transition indices. The photos show examples of nodes of each transition index (TI). The open black circle shows the node traversed. The blue arrow shows the transition, leading from the edge along which ants enter the node, through the node, toward the edge along which they exit. Each transition from an edge to a node to another edge was assigned a transition index with a value between 1 and 4. The lower the transition index, the more likely it is to be traversed by successive ants in the same way, and thus more likely to be reinforced. TI-1 (upper left): a node linking two edges on the same plant; in the example shown, all ants are likely to walk the same way across the top of the branch. TI-2 (upper right): a node that links one plant to another along a trajectory through a node that is likely to be the same for successive ants; in the example shown, most ants are likely to climb up the brown vine from the position shown by the ant approaching the junction from the left. TI-3 (lower left): a node that links one plant to another plant with more than one possible trajectory through the node; in the example shown, ants on the upper vine can reach the lower one either directly or by following the smaller vine that ants in the photo are using. TI-4 (lower right): a node that links one plant to another with many possible trajectories that are often changed by conditions; in the example shown, wind can easily move the leaf so that different ants reach the junction between the leaf and branch, at different places.

131 previous observations of the flow of ants on different edges from a node (e.g., see Fig. 7 in **Gordon**
132 (**2017**)). Each transition through a node in the vegetation (e.g., edge $u \rightarrow v$ through node v to edge
133 $v \rightarrow w$; Methods) was assigned a value of the transition index. A particular node v may have more
134 than one transition index if there were many edges connected to that node.

135

	Tejon 189 Available	Tejon 189 Used	Tejon 446 Available	Tejon 446 Used	Turtle Hill 460 Available	Turtle Hill 460 Used
Edge Length (cm)	10698	20.71 ± 6.21	7615	13.46 ± 0.74	14696	39.97 ± 9.43
Total Nodes	217	43.5 ± 9.43	196	36.09 ± 3.81	202	54.0 ± 17.93
Transition Index	1.60	1.31 ± 0.06	1.70	1.44 ± 0.13	1.48	1.44 ± 0.10
Connectivity	—	3.75 ± 0.23	—	4.00 ± 0.24	—	4.46 ± 0.95

Table 1. Comparison of observed and available networks within the vegetation for the three colonies observed. Values for 'Available' are for all of the vegetation mapped. Values for 'Used' are means, averaged over observation days, for the paths used in each colony's network ($n = 10$ for Tejon 189 and Turtle Hill 460, and $n = 11$ for Tejon 446). Connectivity is a measure of the smallest number of nodes needed to get back to the trail used by the ants from an edge off the trail, averaged over all edges that lead off the trail used by the ants (Methods).

136 **Mapping and modeling turtle ant trail networks**

137 To determine what objectives are optimized by the ants' choice of paths within the vegetation
138 (Figure 2A), we mapped the trail networks that connected the nests and naturally occurring,
139 ephemeral food sources of three colonies (Tejon 189, Tejon 446, Turtle Hill 460), for 10–15 days over
140 the course of 6 weeks, in a tropical dry forest at La Estación Biológica de Chamelea in Jalisco, Mexico.
141 We visually tracked the path taken by the ants and identified each node or junction in the vegetation,
142 where an ant had a choice among more than one edge in the direction it is traveling, as well as the
143 edges between nodes. We measured the length of each edge. We assigned a transition index to
144 each each transition from one edge through a node to another edge, to estimate how likely were
145 successive ants to take the same trajectory through the node and thus reinforce it with pheromone.
146 To evaluate how the ants choose nodes and edges from the options provided by the surrounding
147 vegetation, we also mapped all nodes, measured all edges, and assigned transition indices, for all
148 possible paths up to five nodes away from each node used by the ants. A trail network on one day
149 is illustrated in Figure 2B–C.

150 We modeled the network of vegetation as a directed, weighted graph, $G = (V_G, E_G)$, where each
151 junction forms a node, and edges represent stems or branches that connect one node to another.
152 Edge weights correspond to physical length. Node weights, which are used in some variants of the
153 Steiner tree problem (Byrka *et al.*, 2016; Bateni *et al.*, 2018), correspond to transition indices. We
154 modeled transition indices by converting G into its corresponding line graph (Methods). The nodes
155 corresponding to the nests and food sources were designated as terminals. We compared the
156 extent to which each observed network on a given day optimized each of the 3 objectives, relative
157 to a set of 100,000 random networks connecting the same nests and food sources (Methods).

158 **Turtle ant trail networks favor coherent trails over shortest paths**

159 We compared the relation of observed and random networks, testing for differences among
160 objectives, colonies, and for a statistical interaction of objective by colony. We tested the hypothesis
161 that the networks favor coherent trails, and thus minimize the total number of nodes and the
162 average transition index more than they minimize distance traveled.

163 In all three colonies, the ants' networks optimized the maintenance of coherent trails. There
164 were significant differences among objectives in how well observed networks were optimized
165 by observed relative to random networks (Scheirer-Ray-Hare two-factor ANOVA df 2, $H = 31.718$,
166 $p < 0.001$). Trail networks minimized the average transition index (Dunn test, $Z = 4.395$, $p < 0.001$)
167 and minimized the total number of nodes (Dunn test, $Z = 5.247$, $p < 0.001$), significantly more than
168 the distance traveled (Figure 3A). There were no significant differences between the extent to which

A



B

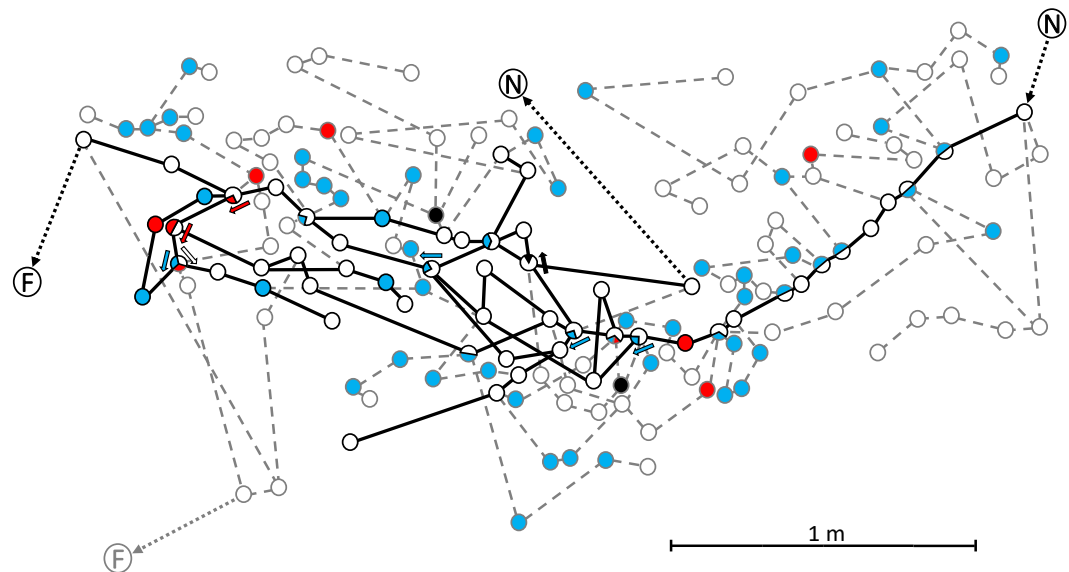


Figure 2. Turtle ant vegetation. A) Vegetation of the network mapped in B, photographed in the dry season before the branches have leaves. B) Illustration of part of the trail network for Tejon 189 on day 9. The figure shows 166 of the 217 nodes mapped in the surrounding vegetation. Edge lengths are scaled to measured distance, but actual location is not represented here. N represents a nest, F represents a food source. Circles represent nodes. Solid lines represent edges used on that day; dashed lines represent edges not used that day (Methods). The color of a node represents the transition index (TI) from the preceding edge to the following one: TI-1, open circles; TI-2, blue; TI-3, red; TI-4, black. At a node where there is a choice of more than one edge in the indicated direction, so that there could be more than one transition taken through a given node, a TI was assigned to each possible transition. For such nodes with more than one transition index, the TI is represented graphically with a pie chart, and arrows show which transition has the TI represented by the arrow's color.

169 observed networks, compared to random ones, minimized the average transition index and the
170 total number of nodes (Dunn test, $Z = 0.852$, ns).

171 Colonies did not differ overall in the relation of observed and random networks for the 3
172 objectives (S-Test, df 2, $H = 2.010$, ns), but there was a significant objective x colony interaction
173 (S-test, df 4, $H = 13.284$, $p < 0.01$). One colony, Turtle Hill 460, differed from the other two colonies in
174 two ways, apparently because of differences in the local vegetation: first, it minimized total nodes,
175 relative to random networks, significantly more than it minimized average transition index (Dunn

C

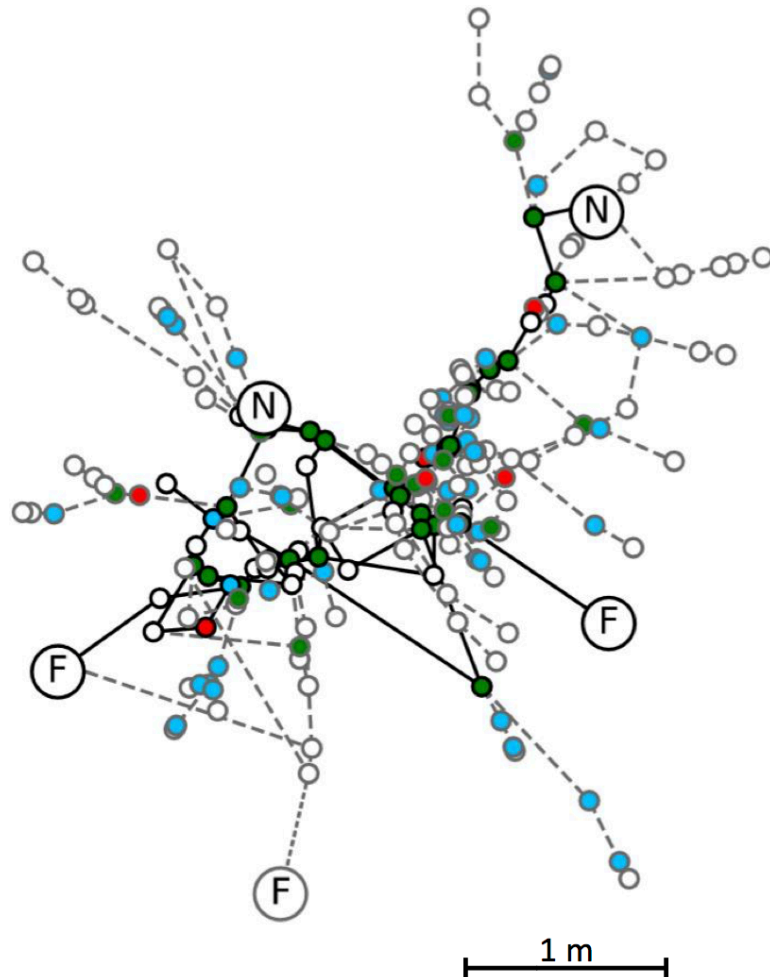


Figure 2. Turtle ant vegetation. C) Map of all 217 nodes for Tejon 189 on day 9. Symbols as in B. The large size of the network makes it difficult to show all TIs per node, so nodes with more than one TI are colored green.

176 test, $Z = 3.347$, $p < 0.05$), and second, it did not minimize average transition index significantly more
177 than average length, relative to random networks (Dunn test, $Z = 1.012$, ns).

178 Random networks with the same number of nodes as the observed network did not differ in
179 total length from the observed network. We tested this to control for the confounding of total edge
180 length and total number of nodes because they are correlated ($R = 0.67$), and to test which one is
181 prioritized when the two objectives give different results. We compared total length in observed
182 and random networks by using a percentile measure (Methods). At 50%, the observed network is
183 equal for the objective to the average random network; the lower the percentile, the better the
184 observed network optimized the objective compared to random networks. In all three colonies,
185 the total length of observed networks was similar to that of the random networks with the same
186 number of nodes: the percentiles were $35.49 \pm 39.57\%$ for Tejon 189, $40.59 \pm 27.65\%$ for Tejon 446,
187 and $34.89 \pm 38.84\%$ for Turtle Hill 460). For all three colonies, the percentile was within one standard
188 deviation of 50%.

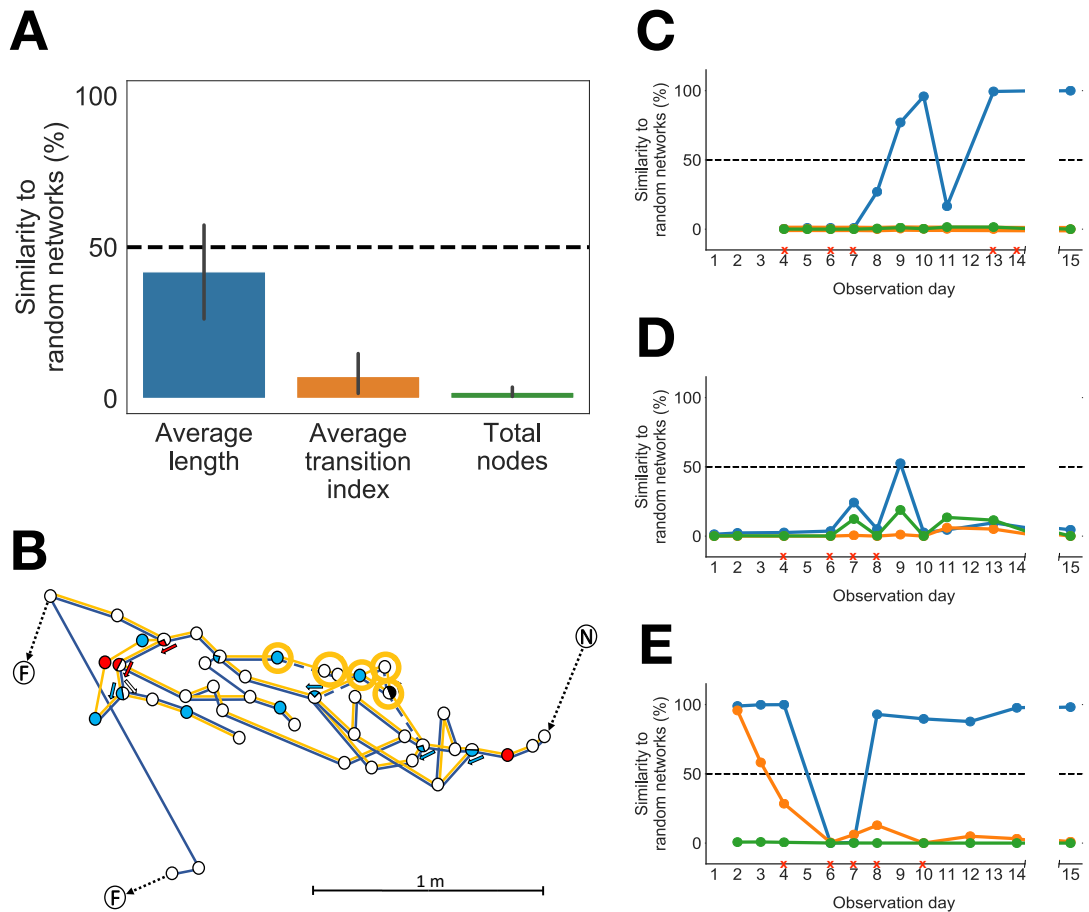


Figure 3. Comparison of random and observed networks. A) Similarity of observed and random networks measured as mean percentile (Methods). A percentile of 50 (dashed line) indicates that the observed network optimized the objective to the same extent as the average random network; the lower the percentile, the better the observed network optimized the objective compared to random networks. Error bars show standard error of the mean. B) Day to day change in trails in Tejon 189, showing a change that decreased both number of nodes and average transition index. Symbols for transition index are the same as in Figure 2B :TI-1, open circles; TI-2, blue; TI-3, red; TI-4, black. Solid yellow lines show trails used on day 9; solid blue lines show trails used on day 10; yellow circles and dashed blue lines show trails linking the six nodes that were used on day 9 but not on day 10. C-E) Day to day changes in mean percentile for each objective. Blue represents average edge length, orange represents average transition index, and green represents total number of nodes. A red 'X' indicates one or more ruptured edges on that day. C, Tejon 189, D, Tejon 446, E, Turtle Hill 460.

189 **Turtle ant trail networks increase coherence over time**

190 From day to day, progressive changes in the trail networks of all three colonies tended to
 191 minimize the average transition index and the total number of nodes more than they minimized
 192 average length (Figure 3B-E). The extent to which average length was minimized varied greatly
 193 from day to day in all three colonies, suggesting that minimizing this objective was not a strong
 194 priority. Figure 3B shows an example of a day-to-day change that minimized both the number of
 195 nodes and average transition index. From day 9 to day 10, the network changed from the path
 196 shown in yellow to the path shown in blue, thus eliminating the 6 nodes circled, including 2 nodes
 197 with TI-2 and one node of TI-4, in favor of a path with nodes all of TI-1 (Figure 3B). Overall, trails
 198 in Tejon 189 (Figure 3C) consistently minimized the total number of nodes and average transition
 199 index but twice increased the average length (days 7 to 10 and 11 to 15). Similarly, in Tejon 446
 200 (Figure 3D), trails progressively decreased the total number of nodes and average transition index,
 201 but increased average length from days 6 to 7, 8 to 9, and 11 to 13. In Turtle Hill 460 (Figure 3E), the
 202 network consistently minimized the total number of nodes. This trail network shifted nests and

203 food sources, and the change led to lower transition indices (days 2 to 10). There was an initial
204 decrease in average edge length (days 4 to 7), due to a rupture on day 6 of a node leading to a 95
205 cm edge, one of the longest edges we measured, rather than to a choice of shorter edges, and then
206 the trails increased in average edge length (days 7 to 14). These day-to-day changes indicate that
207 the networks do not consistently minimize the distance traveled.

208 **Turtle ants form loops to promote coherence**

209 Turtle ants form loops in their paths, consisting of small, temporary alternative paths with the
210 same start and end points, and over time, all but one of these paths tends to be pruned away (*Gordon*,
211 *2017*). Loops are often considered to decrease the efficiency of routing networks (*Alwan and*
212 *Agarwal, 2009; Chouikhi et al., 2015*), but may increase robustness by offering alternative paths if
213 links are broken. Here we hypothesize that loops may occur because trails tend to form along easily
214 reinforced nodes, and some sequence of easily reinforced nodes may naturally form a cycle in the
215 graph.

216 Compared to available loops with the same start and end points (Methods), the observed loops
217 tended to use nodes with low transition indices, and tended to minimize the number of nodes.
218 We compared the centered ranks (Methods) of the average transition index, number of nodes,
219 and average edge length, of paths connecting the same two start and end points on each trail in
220 observed and available loops. A negative value of centered rank indicates that an observed path
221 has a low transition index compared to all of the random paths within the available vegetation with
222 the same start and end points. The mean (SD) of the centered rank in observed loops for average
223 transition index was -1.59 (2.96); for number of nodes was -1.88 (2.91) and for average edge length
224 was 0.44 (2.23); in all cases, significantly different from 0 (T-Test, $|T| > 3$, $p < 0.01$). These results
225 suggest that loop formation in trails may occur as a consequence of selecting trails that have lower
226 transition indices, thus promoting coherence.

227 **Discussion**

228 The trail networks of arboreal ants show how evolution shapes biological distributed algorithms
229 to respond to dynamic environments. Minimizing distance traveled is often considered the main
230 objective in wireless routing algorithms and ant colony optimization (*Di Caro and Dorigo, 1998;*
231 *Dorigo and Blum, 2005; López-Ibáñez et al., 2015*), since rapid communication is often needed
232 between any two nodes in the network. We showed that the trail networks of turtle ants instead
233 optimize the maintenance of a coherent trail by minimizing the total number of nodes, and by
234 minimizing the average transition index; optimizing the latter objective, we show, is NP-complete
235 (Methods). In previous work (*Chandrasekhar et al., 2018*), we proposed a model for the algorithm
236 used to maintain and repair networks. This algorithm did not distinguish between minimizing
237 the number of nodes and the distance traveled, since each edge had equal length. Our results
238 here show that further work is needed to develop an algorithm that captures the role of physical
239 variation in the environment.

240 Minimizing the transition index and the number of nodes contributes to maintaining the coherence
241 of the trail because both diminish the risk of losing ants from the trail. Like water flowing over
242 a rocky stream bed, turtle ants tend to find trails most conducive to the flow of ants. By avoiding
243 nodes with high transition indices, turtle ants reduce the chances of ants wandering off the path
244 and laying pheromone trail that can lead other ants also to leave the trail. Nodes with transition
245 indices of 1 keep the trail on the same plant (*Gordon, 2017*). The vines and trees of the tropical dry
246 forest tend to have long internode distances to reach the sunlight at the edge of the canopy (*Olson*
247 *et al., 2009*). By staying on the same plant, ants are also led to resources at the edge of the canopy,
248 such as flowers that provide nectar.

249 The trail networks must also balance the tradeoff between exploration and coherence. Exploration
250 is necessary for the colony to construct trails (*Sumpter and Beekman, 2003; Garnier et al.,*
251 *2009; Cook et al., 2014; Latty et al., 2011; Garnier et al., 2013; Bouchebti et al., 2019*), search for

252 new resources (*Emek et al., 2015; Feinerman and Korman, 2017; Stickland et al., 1995; Britton*
253 *et al., 1998; Monmarché et al., 2000; Countryman et al., 2015*) and repair breaks (*Gordon, 2017;*
254 *Chandrasekhar et al., 2018; Cabanes et al., 2014*), and the connectivity of the vegetation (Table 1)
255 sets the probability that ants that leave the trail will return to another node on the trail. There
256 appears to be a constant probability of exploration at each node (*Gordon, 2017; Chandrasekhar*
257 *et al., 2018*), so the probability of leaving the trail accumulates with more nodes traversed. Thus,
258 minimizing the number of nodes traversed reduces opportunities for the ants to get lost.

259 Our results here suggest that, as in engineered networks (*Byrka et al., 2016; Bateni et al., 2018*),
260 the cost of including a node in the turtle ant network may vary among nodes, because whether
261 other ants follow an exploring ant that leaves the trail at that node depends on the node's physical
262 configuration. The costs of additional nodes include the loss of ants from the trail, and the pursuit of
263 fruitless paths, which may detract from the colony's ability to distribute resources among its many
264 nests, and make fewer ants available to recruit effectively when a new food source is discovered. In
265 addition, each node provides opportunities for encounters with other, competing species traveling
266 in the same vegetation (*Yanoviak and Kaspari, 2000; Vandermeer et al., 2008; Philpott et al., 2008*).
267 Further work is needed to examine variation among colonies (*Jandt and Gordon, 2016*) in how well
268 they minimize the number of nodes, to learn how selection may shape the process that determines
269 how a trail network is constructed and maintained.

270 Finally, are there useful applications of the principle that variation in the environment provides
271 useful constraints on routing network design? Evolved algorithms operating in the natural world can
272 use structure in the environment to enhance coordination among distributed agents (*Werfel et al.,*
273 *2014*). In engineering, taking into account the physical structure of the environment may improve
274 the design of routing algorithms (*van Rees et al., 2017; Qi et al., 2019; Bajaj and Agrawal, 2004;*
275 *Munguia et al., 2012; Pavone et al., 2010*), for example, by reducing the search space of possible
276 routing paths and steering network construction away from parts of the terrain that are difficult
277 to reach. This could be beneficial in applications such as robot swarms, where distributed agents
278 must coordinate in complex environments using a communication backbone to explore new terrain,
279 exploit of temporary resources, and maintain security against intruders (*Duan et al., 2019*).

280 Materials and Methods

281 Observation of trail networks

282 The trail networks of three turtle ant colonies (Turtle Hill 460, Tejon 446, and Tejon 189) were
283 observed between 06/20/18 and 08/03/18 at La Estación Biológica de Chamelea in Jalisco, Mex-
284 ico. Tejon 189 was observed for 10 days from 6/22/2018–6/28/2018 and again on 07/01/2018,
285 7/04/2018 and 8/3/2018. Tejon 446 was observed for 11 days on 6/20/2018–6/28/2018 and again
286 on 07/01/2018, 07/04/2018, and 08/03/2018; and Turtle Hill 460 was observed for 10 days from
287 06/21/2018–06/28/2018 and again on 07/02/2018, 07/05/2018, and 08/03/2018. Not every net-
288 work was observed on each day. The colonies appeared to be of about the same size, based on
289 observations in comparison with previous work in which size was estimated with mark-recapture
290 measures (*Gordon, 2012*), but here we did not measure colony size.

291 The numbers of observation days were 10 for Tejon 189 and Turtle Hill 460, and 11 for Tejon 446,
292 for a total of $93 = (10 + 10 + 11) \times 3$ observed networks.

293 Networks were mapped using the same methods as in prior work (*Gordon, 2017*), using visual
294 inspection of the paths the ants took through the vegetation. We mapped each node and edge
295 traversed by ants and all possible paths up to 5 nodes away from each node traversed by ants.
296 Each node was assigned a number, and enough nodes were marked, with small labels or stickers
297 on a dead end branch near the node, to identify all same nodes the next day. The initial map of
298 a colony's trail network included all nodes used by the ants, and all nodes up to 5 nodes from
299 each node on the path. The length of each edge was measured with a ruler, including each edge
300 connecting the nodes on the ants path and all nodes up to 5 nodes from each node on the ants'

301 path. A transition index was assigned corresponding to each pair of edges entering and leaving
302 a node. The assignment of a transition index was based on a visual estimate of the number of
303 different trajectories that were available for ants to traverse the node. We were not able to make
304 any direct measurement of the amount of pheromone deposited.

305 The assignment of the transition index was made using the following criteria:

- 306 • TI-1 (Figure 1A): a node linking two edges on the same plant.
- 307 • TI-2 (Figure 1B): a node that links one plant to another along a trajectory through a node that
308 is likely to be the same for successive ants.
- 309 • TI-3 (Figure 1C): a node that links one plant to another plant with more than one possible
310 trajectory through the node.
- 311 • TI-4 (Figure 1D): a node that links one plant to another with many possible trajectories that is
312 often changed by conditions such as the wind.

313 In each day of observation, we recorded which edges and nodes were used by the ants. As
314 observed previously (illustrated for a different set of 3 colonies (*Gordon, 2017*)), each colony's trail
315 network changed which nodes it used from day to day, although each day's path conserved some
316 parts of the previous day's. In the course of the observations reported here, the path of the ants
317 never went outside the range of the 5 nodes around the trail that were originally mapped. The
318 number of nodes and edges observed in each network is shown in Table 1.

319 **Assigning directionality to edges**

320 Experiments with marked ants show that ants tend to use particular routes from a nest (*Gordon,*
321 *2012*), and tend not to turn around on the trail. To account for this, for all edges we defined a
322 direction relative to one terminal; the outbound direction went away from it, and the inbound
323 direction went towards it. We restricted the analysis to paths that proceed in the outbound direction.

324 **Modeling the transition index as a line graph**

325 The transition index of a node describes the probability that successive ants will take the same
326 trajectory from an edge (u, v) through node v to edge (v, w) . Thus, a transition index involving node
327 v depends on which incoming edge was used to reach v , and which outgoing edge was used to
328 leave v .

329 To model the transition index, we used the line graph of G , where $L_G = (V_L, E_L)$. The nodes
330 $V_L = E_G$, and the edges $E_L = \{((x, y), (y, z)) | (x, y), (y, z) \in E_G\}$. The line graph creates a node for each
331 edge in G and connects two nodes if they correspond to two adjacent edges in G . Every edge in
332 the line graph denotes a transition in the original graph; traversing the edge $((u, v), (v, w)) \in L_G$
333 corresponds to starting at u , going to v , crossing the junction at v , and then going to w . We assigned
334 every edge in L a transition index. Figure 4 illustrates this process. The line graph is used to
335 compare the observed and random networks, as described below.

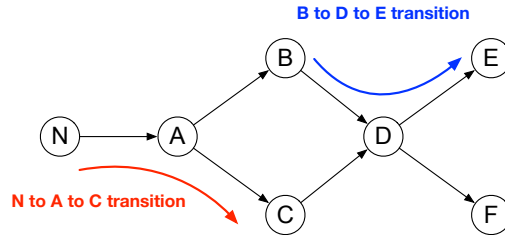
336 **Generating random trail networks**

337 We compared the observed trail networks to random trail networks based on their average edge
338 length, total number of nodes, and average transition index. The random networks were simulated
339 in the graph made from the map of the paths used by ants and the surrounding vegetation up to
340 five nodes from the nodes used by the ants. The measures of number of nodes, edge length and
341 transition index were those measured in the vegetation. The random trail networks may include
342 loops, as did the observed networks.

343 We generated random trail networks as follows:

- 344 1. **Input:** Graph $G = (V_G, E_G)$, terminals $X \subseteq V_G$.
- 345 2. Create an empty graph R ; add a random terminal $x \in X$ to R .
- 346 3. Choose a random terminal $x' \in X$ that has not already been added to R .
- 347 4. Perform a random walk on G that starts at x' and stops when it touches any node in R .

A Original Graph



B Line Graph

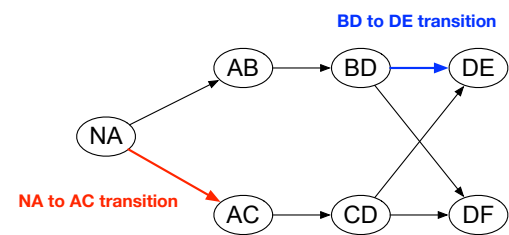


Figure 4. Converting the network to the line graph. A) Original graph. Nodes correspond to junctions in the vegetation, and edges correspond to links, such as a branch or stem, between junctions. B) Line graph. Every edge in the original graph has a corresponding node in the line graph. Two nodes are connected in the line graph if they correspond to two adjacent edges in the original graph. Transitions in the original graph used in this example are highlighted in red and blue.

348 5. Add all edges and nodes touched by the random walk to R .
 349 6. Repeat steps 3–5 until all terminals have been added to R .

350 Comparing observed and random networks

351 To compare the observed and random networks, we computed for each network, using the line
 352 graph (Figure 4), the following three objectives: 1) Average edge length: the average length of all
 353 edges in the network; 2) Total number of nodes: the total number of nodes in the network; and 3)
 354 Average transition index: the average transition index over all transitions in the network.

355 For each objective, we computed a value of φ_{ants} for the observed network and $\varphi_1, \varphi_2, \dots, \varphi_n$
 356 for the n random networks. We measured the similarity between the observed network and the
 357 random networks for that objective as the percentage of random networks that have a lower value
 358 for the objective:

$$100 \times \frac{|\{\varphi_i | \varphi_i \leq \varphi_{\text{ants}}\}|}{n}. \quad (1)$$

359 An observed network is most similar to a random network when its percentile is 50. The closer
 360 the percentile is to 0, the better the observed network optimized the objective, and the closer the
 361 percentile is to 100, the better the random network optimized the objective. This percentile-based
 362 approach is unit-less, making it possible to compare performance for objectives that differ in the
 363 range of values.

364 We treated each comparison of the observed and simulated paths, drawn from observations on
 365 a given day, as independent, because we compared each day's path to a set of randomly generated
 366 paths using the same number of nodes. The relation between the randomly generated paths and
 367 the observed paths for each day was independent of those on any other day. We did not compare
 368 the observed paths from one day to those of another day. The path used by the ants on one day
 369 was similar to the one used by the ants on the previous day, perhaps because of the effect of the
 370 transition indices which generally remained the same from day to day.

371 For each colony (Tejon 189, Tejon 446, Turtle Hill 460), and for each objective (average length,
 372 total nodes, and average transition index), we computed the similarity of each observed network to
 373 100,000 random networks that connected the same set of terminals, using Equation (1).

374 Because the total number of nodes and the total edge length are correlated, we did not
 375 simultaneously compare total length and total number of nodes between random and observed
 376 trail networks. Instead, we tested whether there was a statistically significant difference in total
 377 length between observed and random trail networks with the same number of nodes. For each
 378 observation of one colony on one day, we found all the randomly generated networks that had
 379 the same number of nodes as that observed network (209 for Tejon 189, 1420 for Tejon 446, 221
 380 for Turtle Hill). We then found the total lengths of all of these networks, and used Equation (1) to

381 evaluate how well each observed network optimized total length compared to random networks
382 with the same number of nodes.

383 **Comparision of objectives and colonies**

384 We used the non-parametric Scheirer-Ray-Hare two-factor ANOVA test (*Scheirer et al., 1976*)
385 to test for effects of objective, colony, and the colony x objective interaction on the percentiles of
386 the observed networks compared to random networks. We then applied post hoc Dunn's non-
387 parametric tests (*Ogle et al., 2018*), using a Bonferroni correction for multiple comparisons, with a
388 significance threshold of $p = 0.05$.

389 **Loops**

390 We compared the average transition index and number of nodes in observed loops with loops
391 that were available in the underlying vegetation. A loop was defined as two or more outbound paths
392 that start and end at the same source and target nodes. For each observed loop, we computed all
393 possible paths in the vegetation between the corresponding source and target nodes. We ranked
394 all paths based on the average transition index of the path, and compared this to the rank of the
395 average transition index of the paths used by the ants. We repeated the same measure for total
396 number of nodes and average edge length.

397 We computed the *centered rank* of each path used by the ants as follows: We ranked n available
398 paths in the vegetation, by the average transition index of nodes in the path, total number of nodes
399 in the path, or average length of edges in the path. The ranks of the paths are $1, 2, 3, \dots, n$, and the
400 median rank is $r_m = (n+1)/2$. For each observed path, we computed its centered rank by subtracting
401 the median rank from that path's rank. Using average transition index as an example, the centered
402 rank is 0 when the observed loop had the same average transition index as the median random
403 loop, negative when the observed loop has a lower average transition index, and positive when the
404 observed loop has a higher average transition index. We performed a similar analysis for the total
405 number of nodes and average edge length.

406 **Connectivity**

407 To calculate the connectivity of the vegetation (Table 1), we estimated how many nodes are
408 required for an ant that leaves the trail to return to the trail. For each edge (u, v) connecting a node
409 on the trail to a node off the trail, we found the length, in number of nodes, of the path with fewest
410 nodes from v back to a node on the trail. We measured connectivity as the smallest number of
411 nodes in a path back to the trail, averaged over all edges (u, v) leading off the trail on all days.

412 **Optimizing transition index is NP-complete**

413 Here we show that the problem of constructing the foraging network that connects a given set
414 of terminals while minimizing the average transition index of the network is NP-complete. To do
415 this, we start by showing that finding the minimum average-weight path between two vertices in a
416 graph is NP-complete. In this problem, we are given a graph $G = (V_G, E_G)$ and two vertices $u, v \in V$.
417 The goal is to find a path $\mathcal{P} = [(u, r_1), (r_1, r_2), \dots, (r_k, r_{k+1}), (r_{k+1}, v)]$ that minimizes the average edge
418 length: $\frac{1}{|\mathcal{P}|} \sum_{e \in \mathcal{P}} w(e)$, where $w(e)$ defines the length of edge e . This problem differs from the classic
419 shortest path problem, which seeks a path with minimal total edge length.

420 The standard method for considering the complexity class of an optimization problem is to
421 consider the equivalent decision version of the problem: given a graph $G = (V_G, E_G)$, two vertices
422 $u, v \in V_G$, and an integer k , we ask: is there a path from u to v whose average weight is $\leq k$?

423 **Lemma 1.** *Finding the minimum average-weight path is NP-Complete.*

424 *Proof.* First, we show that this problem is in the class NP. If we are given a path from u to v , we can
425 verify that the path is a valid u - v path, and that the average edge weight is $\leq k$. This certificate will
426 clearly be of polynomial length, and we can verify that it is correct in polynomial time.

427 Next, we show that the problem is NP-hard. We proceed via reduction from the Hamiltonian
428 path problem, which is NP-Complete. Given a directed graph $G = (V_G, E_G)$, the directed Hamiltonian
429 path problem seeks a path that touches every vertex $v \in V_G$ exactly once. We construct a graph G'
430 as follows: G' contains all of the vertices in G along with two additional vertices, s and t . We assign
431 a weight of 1 to all of the original edges in G . We add a directed edge from s to every vertex $v \in V_G$,
432 and we add a directed edge from every vertex $v \in V_G$ to t . We assign a weight of 2 to all edges that
433 include either s or t .

434 The smallest possible average edge weight for any path from s to t is $\frac{3 + |V_G|}{|V_G| + 1}$, and such a path
435 exists if and only if G has a directed Hamiltonian path.

436 The reduction requires adding 2 new nodes, and $2|V|$ new edges to G . Thus the reduction clearly
437 takes only polynomial time. \square

438 We now use Lemma 1 to show that optimizing average transition index is NP-Complete. Let
439 $L = (V_L, E_L)$ be a graph whose edge weights correspond to transition indices, which we represent
440 using the line graph (Figure 4). Given a set of terminals $X \subseteq V_L$, we seek to find a subtree $F_X \subseteq L$ that
441 minimizes the average value of all edge weights in F_X . We require that F_X be connected without
442 cycles to represent the fact that cycles in turtle ant trails are typically pruned.

443 Once again we consider the decision problem: given a line network $L = (V_L, E_L)$, a set of
444 terminals X , and an integer k , does L contain a subtree F_X whose average weight is $\leq k$?

445 **Lemma 2.** *Finding the subtree F_X that optimizes average transition index is NP-Complete.*

446 *Proof.* First, we prove that the problem is in NP. Given V_L, X, k , if we are presented with a subgraph
447 F_X as a certificate, we can verify that F_X is a valid solution. We check that F_X is valid subgraph,
448 that F_X is connected, that F_X contains every terminal node X , and that the average weight of the
449 edges in F is $\leq k$. Clearly the size of F_X is polynomially bounded, and we can verify that F_X is a valid
450 solution in polynomial time.

451 To show that the problem is NP-hard, we proceed via reduction from the minimum average-
452 weight path problem above. Given G and vertices u and v , we simply treat G as the line graph
453 (L), and designate terminals $X = \{u, v\}$; this means F_X is simply a u - v path. We seek the trail that
454 optimizes the average transition index between terminals u and v . By construction, this is the
455 minimum average-weight path from u to v in the line graph, meaning there is a subgraph F_X with
456 average weight of $\leq k$ if and only if the original graph has a u - v path with average edge weight $\leq k$.
457 Further, the reduction clearly takes only polynomial time. \square

458 Acknowledgements

459 We thank Ibai Zabaleta and especially Taggart Butterfield for assistance in the field; and Daniel
460 Beck, Katharine Renton, and the staff at the Estación Biológica de Chamela for their help. We are
461 grateful for the comments of anonymous reviewers of a previous version of the manuscript.

462 Funding

463 The work was supported by a grant from the CISCO Research Fund to DMG, a grant from the
464 National Science Foundation under award CAREER DBI-1846554 to SN, a grant from the National
465 Science Foundation under award 1559447 to Daniel Beck that supported field work for CA, funding
466 from Chapman Foundations Management, LLC, to AC, and by the European Research Council (ERC)
467 under the European Union's Horizon 2020 research and innovation programme (grant agreement
468 number 647704 to JARM).

469 Author Contributions

470 AC: data analysis, computational modeling, manuscript preparation. JARM: computational mod-
471 eling, manuscript preparation. CA: data collection, manuscript preparation. SN: data analysis,

472 computational modeling, manuscript preparation. DMG: data collection, data analysis, computa-
473 tional modeling, and manuscript preparation.

474 Competing Interests

475 None of the authors have competing interests.

476 Data Availability Statement

477 All data collected and analyzed will be archived at Stanford Digital Repository at the Stanford
478 Libraries. Python code is available at: <https://github.com/DiODeProject/SteinerAnts>.

479 References

480 **Alwan H**, Agarwal A. A survey on fault tolerant routing techniques in wireless sensor networks. In: *2009 Third
481 International Conference on Sensor Technologies and Applications* IEEE; 2009. p. 366–371.

482 **Aron S**, Pasteels JM, Deneubourg JL. Trail-laying behaviour during exploratory recruitment in the argentine ant,
483 *Iridomyrmex humilis* (Mayr). *Biology of Behaviour*. 1989; 14:207–217.

484 **Bajaj R**, Agrawal DP. Improving scheduling of tasks in a heterogeneous environment. *IEEE Transactions on
485 Parallel and Distributed Systems*. 2004; 15(2):107–118.

486 **Bateni MH**, Hajighayi MT, Liaghat V. Improved Approximation Algorithms for (Budgeted) Node-weighted
487 Steiner Problems. *SIAM Journal on Computing*. 2018; 47(4):1275–1293.

488 **Bottinelli A**, van Wilgenburg E, Sumpter DJ, Latty T. Local cost minimization in ant transport networks: from
489 small-scale data to large-scale trade-offs. *Journal of the Royal Society Interface*. 2015; 12(112):20150780.

490 **Bouchebti S**, Travaglini RV, Forti LC, Fourcassié V. Dynamics of physical trail construction and of trail usage in
491 the leaf-cutting ant *Atta laevigata*. *Ethology Ecology & Evolution*. 2019; 31(2):105–120.

492 **Britton N**, Stickland T, Franks N. Analysis of ant foraging algorithms. *Journal of Biological Systems*. 1998;
493 6(04):315–336.

494 **Buhl J**, Hicks K, Miller ER, Persey S, Alinvi O, Sumpter DJ. Shape and efficiency of wood ant foraging networks.
495 *Behavioral Ecology and Sociobiology*. 2009; 63(3):451–460.

496 **Byrka J**, Lewandowski M, Moldenhauer C. Approximation algorithms for node-weighted prize-collecting Steiner
497 tree problems on planar graphs. *arXiv preprint arXiv:160102481*. 2016; .

498 **Cabanes G**, van Wilgenburg E, Beekman M, Latty T. Ants build transportation networks that optimize cost and
499 efficiency at the expense of robustness. *Behavioral Ecology*. 2014; 26(1):223–231.

500 **Chandrasekhar A**, Gordon DM, Navlakha S. A distributed algorithm to maintain and repair the trail networks
501 of arboreal ants. *Sci Rep*. 2018 6; 8(1):9297.

502 **Chandrasekhar A**, Navlakha S. Neural arbors are Pareto optimal. *Proc Biol Sci*. 2019 05; 286(1902):20182727.

503 **Cherix D**, Werner P, Catzeflis F, et al. Spatial organisation of a polycalic system in *Formica* (Coptoformica)
504 *exsecta* Nyl. (Hymenoptera: Formicidae). *Mitteilungen der Schweizerischen Entomologischen Gesellschaft*.
505 1980; 53(2/3):163–172.

506 **Chouikhi S**, El Korbi I, Ghamri-Doudane Y, Saidane LA. A survey on fault tolerance in small and large scale
507 wireless sensor networks. *Computer Communications*. 2015; 69:22–37.

508 **Colorni A**, Dorigo M, Maniezzo V, et al. Distributed optimization by ant colonies. In: *Proceedings of the first
509 European conference on artificial life*, vol. 142 Paris, France; 1991. p. 134–142.

510 **Conn A**, Pedmale UV, Chory J, Navlakha S. High-resolution laser scanning reveals plant architectures that reflect
511 universal network design principles. *Cell systems*. 2017; 5(1):53–62.

512 **Cook Z**, Franks DW, Robinson EJ. Efficiency and robustness of ant colony transportation networks. *Behavioral
513 ecology and sociobiology*. 2014; 68(3):509–517.

514 **Countryman SM**, Stumpe MC, Crow SP, Adler FR, Greene MJ, Vonshak M, Gordon DM. Collective search by ants
515 in microgravity. *Frontiers in Ecology and Evolution*. 2015; 3:25.

516 **Couzin ID**, Franks NR. Self-organized lane formation and optimized traffic flow in army ants. Proceedings of the
517 Royal Society of London Series B: Biological Sciences. 2003; 270(1511):139–146.

518 **Couzin ID**, Krause J, Franks NR, Levin SA. Effective leadership and decision-making in animal groups on the
519 move. Nature. 2005; 433(7025):513.

520 **Deneubourg JL**, Aron S, Goss S, Pasteels J, Duerinck G. Random behaviour, amplification processes and number
521 of participants: how they contribute to the foraging properties of ants. Physica D: Nonlinear Phenomena.
522 1986; 22(1):176–186.

523 **Deneubourg JL**, Goss S, Franks N, Pasteels J. The blind leading the blind: modeling chemically mediated army
524 ant raid patterns. Journal of insect behavior. 1989; 2(5):719–725.

525 **Di Caro G**, Dorigo M. AntNet: Distributed stigmergetic control for communications networks. Journal of Artificial
526 Intelligence Research. 1998; 9:317–365.

527 **Dorigo M**, Blum C. Ant colony optimization theory: A survey. Theoretical Computer Science. 2005 9; 344(2-
528 3):243–278. <http://dx.doi.org/10.1016/j.tcs.2005.05.020>, doi: 10.1016/j.tcs.2005.05.020.

529 **Dorigo M**, Stützle T. Ant Colony Optimization. Cambridge, MA: MIT Press; 2004.

530 **Duan X**, George M, Patel R, Bullo F. Robotic Surveillance Based on the Meeting Time of Random Walks. arXiv
531 preprint arXiv:191202693. 2019; .

532 **Dussutour A**, Fourcassie V, Helbing D, Deneubourg JL. Optimal traffic organization in ants under crowded
533 conditions. Nature. 2004; 428(6978):70–73.

534 **Eberhart RC**, Kennedy J, et al. A new optimizer using particle swarm theory. In: *Proceedings of the sixth
535 international symposium on micro machine and human science*, vol. 1 New York, NY; 1995. p. 39–43.

536 **Emek Y**, Langner T, Stoltz D, Uitto J, Wattenhofer R. How many ants does it take to find the food? Theoretical
537 Computer Science. 2015; 608:255–267.

538 **Fei Z**, Li B, Yang S, Xing C, Chen H, Hanzo L. A survey of multi-objective optimization in wireless sensor networks:
539 Metrics, algorithms, and open problems. IEEE Communications Surveys & Tutorials. 2016; 19(1):550–586.

540 **Feinerman O**, Korman A. The ANTS problem. Distributed Computing. 2017; 30(3):149–168.

541 **Flanagan TP**, Pinter-Wollman NM, Moses ME, Gordon DM. Fast and flexible: Argentine ants recruit from nearby
542 trails. PloS one. 2013; 8(8):e70888.

543 **Franks NR**. Army ants: a collective intelligence. American Scientist. 1989; 77:138–145.

544 **Gambardella LM**, Montemanni R, Weyland D. Coupling ant colony systems with strong local searches. European
545 Journal of Operational Research. 2012; 220(3):831–843.

546 **Garnier S**, Combe M, Jost C, Theraulaz G. Do ants need to estimate the geometrical properties of trail bifurcations
547 to find an efficient route? A swarm robotics test bed. PLoS computational biology. 2013; 9(3):e1002903.

548 **Garnier S**, Guérécheau A, Combe M, Fourcassie V, Theraulaz G. Path selection and foraging efficiency in
549 Argentine ant transport networks. Behavioral Ecology and Sociobiology. 2009; 63(8):1167–1179.

550 **Gong H**, Fu L, Fu X, Zhao L, Wang K, Wang X. Distributed multicast tree construction in wireless sensor networks.
551 IEEE Transactions on Information Theory. 2016; 63(1):280–296.

552 **Gordon DM**. The dynamics of foraging trails in the tropical arboreal ant *Cephalotes goniodontus*. PLoS ONE.
553 2012; 7(11):e50472.

554 **Gordon DM**. The evolution of the algorithms for collective behavior. Cell Syst. 2016 12; 3(6):514–520.

555 **Gordon DM**. The ecology of collective behavior. PLoS Biol. 2014; 12(3):e1001805.

556 **Gordon DM**. Local regulation of trail networks of the arboreal turtle ant, *Cephalotes goniodontus*. The American
557 Naturalist. 2017; 190(6):E156–E169.

558 **Gordon DM**. The ecology of collective behavior in ants. Annual review of entomology. 2019; 64:35–50.

559 **Hein AM**, Brumley DR, Carrara F, Stocker R, Levin SA. Physical limits on bacterial navigation in dynamic
560 environments. J R Soc Interface. 2016 1; 13(114):20150844.

561 **Jandt J**, Gordon D. The behavioral ecology of variation in social insects. *Current opinion in insect science*. 2016; 15:40–44.

563 **Karaboga D**. An idea based on honey bee swarm for numerical optimization. Technical report-tr06, Erciyes university, engineering faculty, computer engineering department; 2005.

565 **Latty T**, Ramsch K, Ito K, Nakagaki T, Sumpter DJ, Middendorf M, Beekman M. Structure and formation of ant transportation networks. *J R Soc Interface*. 2011; 9(62):1298–1306.

567 **Levin D**. The environment constrains successful search strategies in natural distributed systems. . 2016; .

568 **López-Ibáñez M**, Stützle T, Dorigo M. Ant Colony Optimization: A Component-Wise Overview. . 2015; .

569 **Lynch NA**. *Distributed Algorithms*. San Francisco, CA, USA: Morgan Kaufmann Publishers Inc.; 1996.

570 **Malíčková M**, Yates C, Bodová K. A stochastic model of ant trail following with two pheromones. *arXiv:150806816*. 2015; .

572 **Middleton EJ**, Latty T. Resilience in social insect infrastructure systems. *Journal of The Royal Society Interface*. 2016; 13(116):20151022.

574 **Monmarché N**, Venturini G, Slimane M. On how *Pachycondyla apicalis* ants suggest a new search algorithm. *Future generation computer systems*. 2000; 16(8):937–946.

576 **Munguia LM**, Bader DA, Ayguade E. Task-based parallel breadth-first search in heterogeneous environments. In: *2012 19th International Conference on High Performance Computing* IEEE; 2012. p. 1–10.

578 **Nguyen UT**, Xu J. Multicast routing in wireless mesh networks: Minimum cost trees or shortest path trees? *IEEE Communications Magazine*. 2007; 45(11):72–77.

580 **Ogle DH**, Wheeler P, Dinno A. FSA: Fisheries Stock Analysis; 2018, <https://github.com/droglenc/FSA>, r package version 0.8.22.

582 **Olson ME**, Aguirre-Hernández R, Rosell JA. Universal foliage-stem scaling across environments and species in dicot trees: plasticity, biomechanics and Corner's Rules. *Ecology Letters*. 2009; 12(3):210–219.

584 **Pavone M**, Fazzoli E, Bullo F. Adaptive and distributed algorithms for vehicle routing in a stochastic and dynamic environment. *IEEE Transactions on Automatic Control*. 2010; 56(6):1259–1274.

586 **Perna A**, Latty T. Animal transportation networks. *Journal of The Royal Society Interface*. 2014; 11(100):20140334.

587 **Philpott SM**, Perfecto I, Vandermeer J. Behavioral diversity of predatory arboreal ants in coffee agroecosystems. *Environ Entomol*. 2008 Feb; 37(1):181–191.

589 **Powell S**, Costa AN, Lopes CT, Vasconcelos HL. Canopy connectivity and the availability of diverse nesting resources affect species coexistence in arboreal ants. *Journal of Animal Ecology*. 2011; 80(2):352–360.

591 **Prömel HJ**, Steger A. The Steiner tree problem: a tour through graphs, algorithms, and complexity. Springer Science & Business Media; 2012.

593 **Qi L**, Griego AD, Fricke GM, Moses ME. Comparing Physical and Simulated Performance of a Deterministic and a Bio-inspired Stochastic Foraging Strategy for Robot Swarms. In: *Proceedings of the International Conference on Robotics and Automation (ICRA)*. IEEE; 2019. .

596 **van Rees WM**, Vouga E, Mahadevan L. Growth patterns for shape-shifting elastic bilayers. *Proceedings of the National Academy of Sciences*. 2017; 114(44):11597–11602.

598 **Reid CR**, Lutz MJ, Powell S, Kao AB, Couzin ID, Garnier S. Army ants dynamically adjust living bridges in response to a cost–benefit trade-off. *Proceedings of the National Academy of Sciences*. 2015; 112(49):15113–15118.

600 **Scheirer CJ**, Ray WS, Hare N. The analysis of ranked data derived from completely randomized factorial designs. *Biometrics*. 1976; p. 429–434.

602 **Stickland T**, Britton NF, Franks NR. Complex trails and simple algorithms in ant foraging. *Proceedings of the Royal Society of London Series B: Biological Sciences*. 1995; 260(1357):53–58.

604 **Sumpter DJ**, Beekman M. From nonlinearity to optimality: pheromone trail foraging by ants. *Animal behaviour*. 2003; 66(2):273–280.

606 **Tero A**, Takagi S, Saigusa T, Ito K, Bebber DP, Fricker MD, Yumiki K, Kobayashi R, Nakagaki T. Rules for biologically
607 inspired adaptive network design. *Science*. 2010 Jan; 327(5964):439–442.

608 **Tsutsui S**. Ant colony optimization with cunning ants. *Transactions of the Japanese Society for Artificial
609 Intelligence*. 2007; 22:29–36.

610 **Vandermeer J**, Perfecto I, Philpott SM. Clusters of ant colonies and robust criticality in a tropical agroecosystem.
611 *Nature*. 2008; 451(7177):457.

612 **Werfel J**, Petersen K, Nagpal R. Designing collective behavior in a termite-inspired robot construction team.
613 *Science*. 2014 2; 343(6172):754–758.

614 **Wiesemann W**, Stützle T. Iterated ants: An experimental study for the quadratic assignment problem. In: *International Workshop on Ant Colony Optimization and Swarm Intelligence* Springer; 2006. p. 179–190.

615

616 **Wiles TJ**, Jemielita M, Baker RP, Schliemann BH, Logan SL, Ganz J, Melancon E, Eisen JS, Guillemin K, Parthasarathy
617 R. Host gut motility promotes competitive exclusion within a model intestinal microbiota. *PLoS biology*. 2016;
618 14(7):e1002517.

619 **Yanoviak S**, Kaspari M. Community structure and the habitat template: ants in the tropical forest canopy and
620 litter. *Oikos*. 2000; 89(2):259–266.